vuv photoionization of uv-laser-tailored Ni-like Cu $3d^9$ atoms

A. Verweyen,[1,*] A. von dem Borne,[1] P. Glatzel,[1,†] Ph. Wernet,[1] B. Sonntag[1] K. Godehusen,[2]
Ch. Gerth,[2] and P. Zimmermann[2]

[1]*Universität Hamburg, II. Institut für Experimentalphysik, Luruper Chaussee 149, D-22761 Hamburg, Germany*
[2]*Technische Universität Berlin, Institut für Atomare and Analytische Physik, Hardenbergstraβe 36, D-10263 Berlin, Germany*
(Received 26 February 1999)

Cu atoms have been prepared in the Ni-like Cu $3d^9 4s^2$ state by uv-laser pumping. In contrast to the ground-state atoms, the Cu $3d^9 4s^2$ atoms exhibit a prominent asymmetric resonance in the $3d^{-1}$ partial cross section at the $3p$ threshold. A close similarity to the corresponding resonance in the spectrum of Ni $3d^9 4s$ atoms is demonstrated. [S1050-2947(99)50808-1]

PACS number(s): 32.80.Fb, 32.80.Dz

Core-level photoelectron spectroscopy for the element-specific investigation of solids has been greatly enhanced by combining it with electron spin-polarization analysis and the measurement of magnetic dichroism; the ferromagnetic $3d$ transition metals Fe, Co, Ni; and the neighboring elements Cr and Mn, bound on surfaces, in ultrathin films and multilayers, have attracted particular interest ([1–7] and references therein). Corresponding measurements on free oriented metal atoms can yield detailed information on the importance of intra-atomic effects. The extension of the pioneering study on the dichroism of free laser-oriented Cr atoms [8] to Mn-Ni atoms, however, is hampered by experimental difficulties. The strong optical transitions for the laser pumping process lie in the uv below 380 nm. In an approach to this wavelength regime we have successfully implemented a frequency-doubling scheme.

Atomic Ni is probably the most interesting but also the most difficult sample in the Mn-Ni series with respect to the preparation of a laser-oriented atomic beam. At a temperature of 1500 °C, which is required for a vapor pressure of 10^{-2} mm Hg [9], Ni becomes an aggressive melt and must be contained in ceramic, since it alloys with refractory metals. Furthermore, at these elevated temperatures 60% of the Ni atoms are thermally excited, thereby preventing their participation in the optical pumping process. Even worse, half of the Ni atoms are distributed over the two initial configurations $3d^8 4s^2$ and $3d^9 4s$; this enormously complicates the interpretation of the photoelectron spectrum. In order to bypass these difficulties, we prepared a beam of free Cu atoms in an open-$3d$-shell ''Ni-like'' state. The metastable Cu* $3d^9 4s^2$ atoms were investigated with respect to their suitability as a model system for the $3p$ photoionization of free Ni $3d^9 4s$ atoms.

In the experiment a collimated beam of Cu atoms was produced with a high-temperature metal atom furnace [10] by resistively heating a Ta crucible containing the Cu metal to approximately 1250 °C. The atomic beam was intersected by uv-laser radiation and vuv synchrotron radiation propagating in opposite directions. The laser was used to prepare

the Cu atoms in an excited metastable $3d^9$ state, as will be explained below. The $3p$ electrons of the metastable Cu* atoms were then excited with synchrotron radiation from the U1 TGM-6 high-flux undulator station at the electron storage ring BESSY I in Berlin. Photoelectrons emitted at angles close to the magic angle $\Theta_{\text{CMA}} = 54.7°$ relative to the polarization axis of the synchrotron radiation were detected by a 180° cylindrical mirror analyzer (CMA) with an energy resolution of $E_{\text{pass}}/\Delta E_{\text{pass}} = 125$. All electron spectra in this work have been corrected for the analyzer transmission and normalized to the incoming photon flux. The calibration of the photon energy was established by measuring the Xe $4d_{5/2} \rightarrow np$ and Kr $3d_{3/2} \rightarrow np$ resonance positions [11]. More details on the experimental setup can be found in Ref. [12].

The preparation of the metastable Cu* atoms is indicated in Fig. 1. An Ar^+-laser-pumped single-mode cw ring dye laser operated with DCM provided 800 mW at 650 nm and approximately 5–10 % in the second harmonic, generated in an external ring resonator. Note that the hyperfine structure ([13], and references therein) introduced by the nuclear spin $I = 3/2$ is not shown in Fig. 1. In the experiment the strongest $4s \rightarrow 4p_{3/2}$ transition $F = 2 \rightarrow F' = 3$ of the more abundant isotope ^{63}Cu (69%) was excited with a laser bandpass of 1
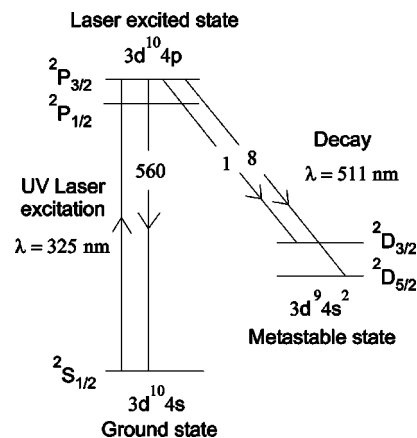

FIG. 1. Illustration of the uv-laser tailoring process in an energy-level scheme. The five lowest fine-structure levels of Cu I are shown. A small fraction of the laser-excited $3d^{10} 4p$ $^2P_{3/2}$ atoms decays into the metastable state $3d^9 4s^2$ by emitting green fluorescence light. The numbers on the arrows give the relative transition probabilities [15].
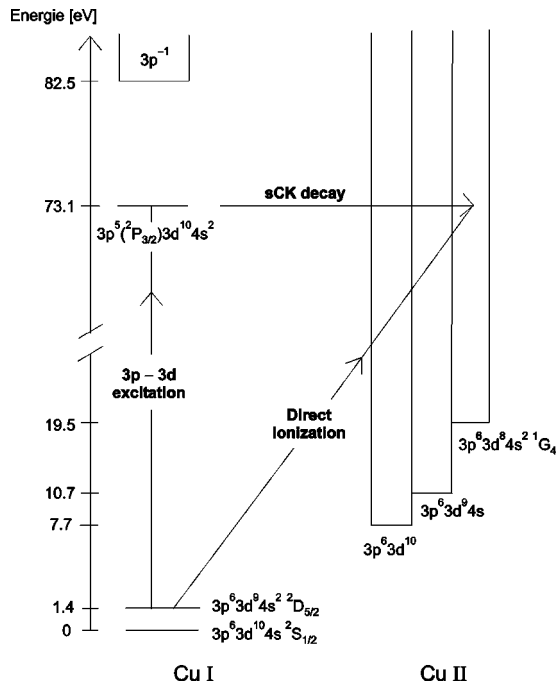
FIG. 2. vuv energy level scheme of Cu atoms. Interference between direct $3d$ photoionization of metastable Cu atoms and $3p$ excitation followed by autoionization is indicated by arrows. The vuv energies are based on high-resolution absorption spectroscopy [16] and photoelectron spectroscopy [17].

FIG. 3. Photoelectron spectrum of Cu atoms in the valence energy region, recorded at a photon energy of $\hbar\omega = 71.9$ eV. The spectrum was taken with the laser radiation tuned to the $4s \rightarrow 4p$ resonance ($-\blacktriangle-$) and without laser radiation ($--\bigcirc--$).

MHz at 325 nm. The laser-excited $3d^{10}4p$ state has a small admixture of $3d^9 4s 4p$ [14] that can decay to the metastable $3d^9 4s^2$ state by a one-electron transition; the corresponding probability (relative to a decay back into the ground state) amounts to $\sim$1% [15]. From the $^2P_{3/2}$ laser-excited state, the $^2D_{5/2}$ metastable state is populated much more effectively than the $^2D_{3/2}$ metastable state (ratio 8:1 [15]); approximately 5–10 % of the atoms could be prepared in the metastable Cu* state.

The inner-shell excitation and decay processes are illustrated in the simplified energy-level diagram of Fig. 2. It displays the excitation of the $3p^5(^2P_{3/2})3d^{10}4s^2$ resonance state at 73.1 eV [16] from the metastable state $3p^6 3d^9(^2D_{5/2})4s^2$. Since for the $3p^5 3d^{10}4s^2$ states the $3d$ shell is filled, there is only the $3p$ core-hole spin-orbit splitting of 2.3 eV [17]. The first $3p^{-1}$ ionization threshold $3p^5(^2P_{3/2})3d^{10}4s$ at 82.5 eV [17] is also depicted. The decay of the $3p^5(^2P_{3/2})3d^{10}4s^2$ resonance by a super Coster-Kronig (sCK)-type autoionization transition into the $3p^6 3d^8(^1G_4)4s^2\varepsilon f$ continuum is marked by an arrow in Fig. 2. Interference between this indirect ionization channel and the direct $3d$ ionization is expected to give rise to an asymmetric Fano-type resonance profile.

The photoelectron spectrum of atomic Cu in the valence energy region, taken at a photon energy of $\hbar\omega = 71.9$ eV, is given by the dashed line connecting the open circles in Fig. 3. The photon energy had been tuned to the $3p_{3/2} \rightarrow 3d$ resonance maximum of the metastable Cu* atoms (see Fig. 2) in order to enhance their weak $3d^{-1}$ photoelectron signal. The dominating feature in Fig. 3 is the $3d^{-1}$ main photoelectron line of Cu atoms in t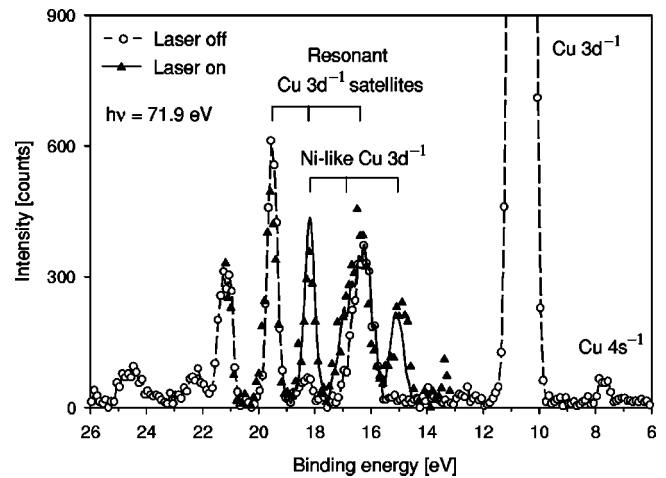he ground state at a binding energy of 10.7 eV, stemming from the $3d^{10}4s \rightarrow 3d^9 4s\varepsilon l$ photoionization process. In comparison, the $4s^{-1}$ main line below 8 eV is hardly visible.

In the energy region from 12 to 20 eV, most of the photoelectron lines are due to multiplet-split $3d^8 4s^2$ final ionic states. Since the ground state and the metastable state have the same parity, the same states can be accessed from them in a dipole transition. The lines observed at binding energies of 16.5, 18.3, and 19.6 eV are resonantly enhanced by the $3p^6 3d^{10}4s\,^2S_{1/2} \rightarrow 3p^5(^2P_{3/2})3d^{10}4s^2 \rightarrow 3p^6 3d^8(^3F,^1D,^1G)4s^2\varepsilon l$ excitation and decay process starting from the Cu ground state [18,19].[1] In the region of 16.0–16.9 eV the $3d^9 4p$ final ionic states also contribute; they are not affected by the $3p$ resonances.

The second set of data shown in Fig. 3 has been taken with laser radiation on (solid triangles approximated by the solid line). In the energy region from 12 to 20 eV, the photoelectron intensity is strongly modified by the laser radiation. The photoelectron lines from the metastable Cu* atoms[2] are shifted by 1.4 eV to lower binding energies, in comparison with the corresponding lines of ground-state Cu atoms. Therefore the Cu* photoelectron lines at 15.1, 16.9, and 18.2 eV in the spectrum taken with the laser radiation on (Fig. 3) are assigned to the same final ionic $3d^8 4s^2$ states ($^3F,^1D,^1G$) discussed above. Starting from the $3d^9 4s^2$ metastable state instead of the ground state, the $3d^8 4s^2$ final ionic states can also be reached simply by the ionization of a $3d$ electron.

The $3d^{-1}$ partial cross section of the Ni-like Cu atoms was measured by recording the intensity variation of the pho-

---

[1]Although the maximum of the $3p^6 3d^{10}4s \rightarrow 3p^5(^2P_{3/2})3d^{10}4s^2$ resonance lies at 73.1 eV [16], it is already excited 1.2 eV lower due to the large lifetime width of $\Gamma_{3p} = 1.8$ eV (full width at half maximum) [20,21].

[2]The $3d^{10}4p \rightarrow 3d^9 4p\varepsilon l$ lines from the short-lived laser-excited atoms expected at binding energies of 12.2–13.1 eV [14] are not included in Fig. 3.

toelectron line at $E_B = 18.2$ eV (see Fig. 3) while scanning the photon energy (CIS spectrum). In order to correct for the contribution of the ground-state atoms, two spectra were taken simultaneously by switching the laser beam on and off for every datum point using a computer-controlled shutter. The difference of these two spectra, which directly gives the $3d^9 4s^2 \rightarrow 3d^8(^1G)4s^2 \varepsilon l$ partial photoionization cross section, is depicted in Fig. 4 (solid points with error bars). The spectrum displays the broad $3p^6 3d^9 4s^2 \rightarrow 3p^5(^2P_{3/2})3d^{10}4s^2$ resonance[3] with a pronounced asymmetry corresponding to a positive Fano q parameter. Similar $3p \rightarrow 3d$ resonances are characteristic of the vuv spectra of the open $3d$-shell transition-metal atoms; they comprise a considerable fraction of the oscillator strength for transitions from the $3p$ subshell [22,23]. The spin-orbit partner state $3p^5(^2P_{1/2})3d^{10}4s^2$ cannot be excited from the metastable state $3d^9(^2D_{5/2})4s^2$ predominantly populated in the laser-tailoring process; excitation from the weakly populated $3d^9(^2D_{3/2})4s^2$ metastable state is not visible in the spectrum of Fig. 4.

For comparison, the $3d^{-1}$ partial photoionization cross section of ground-state Cu $3p^6 3d^{10}4s$ atoms, measured at $E_B = 10.7$ eV (see Fig. 3), is included in Fig. 4 (open circles approximated by the dashed line). It was scaled by a factor of 0.075 (as a result of a fitting procedure; see below), which reflects the small fraction of atoms in the metastable state. The ground-state spectrum, being hardly affected by $3p$ excitations, differs markedly from the spectrum of the metastable state.

The $3p_{3/2} \rightarrow 3d$ resonance in the spectrum of Ni-like Cu atoms can be well approximated by a Fano-type profile (solid line in Fig. 4). The resonance energy of 71.70 eV and the resonance width of 1.84 eV were derived from spectra of ground-state atoms displaying the $3p^6 3d^{10}4s \rightarrow 3p^5(^2P_{3/2})3d^{10}4s^2$ resonance with much better statistics. For the fit of the Fano profile a noninteracting continuum [24] was taken into account that was matched to the ground-state $3d^{-1}$ continuum of Fig. 4; the additional $4s$ electron should not make a large difference. The approximation resulted in an Fano asymmetry parameter of $q = +2.6 \pm 1$; the considerable uncertainty is due to the statistical scatter of the data.

It is very instructive to compare the partial cross section of the Ni-like Cu atoms with the analogous cross section $3p^6 3d^9 4s \rightarrow 3p^6 3d^8(^1G)4s\varepsilon l$ of excited Ni atoms. The corresponding Ni spectrum [25,26] is given by the open diamonds in Fig. 4; it displays a strong asymmetric resonance attributed to a $3p^6 3d^9 4s \rightarrow 3p^5(^2P_{3/2})3d^{10}4s$ excitation. In Fig. 4, the Ni spectrum was shifted by 9 eV to higher energies and the intensity of the Ni resonance was matched to the Ni-like Cu resonance. The shapes of the Ni and the Ni-like Cu resonances are very similar. A detailed inspection reveals that there is possibly a weak contribution from the Ni $3p_{1/2} \rightarrow 3d$ spin-orbit partner on the high-energy side of the $3p_{3/2} \rightarrow 3d$ resonance. The corresponding splitting would be
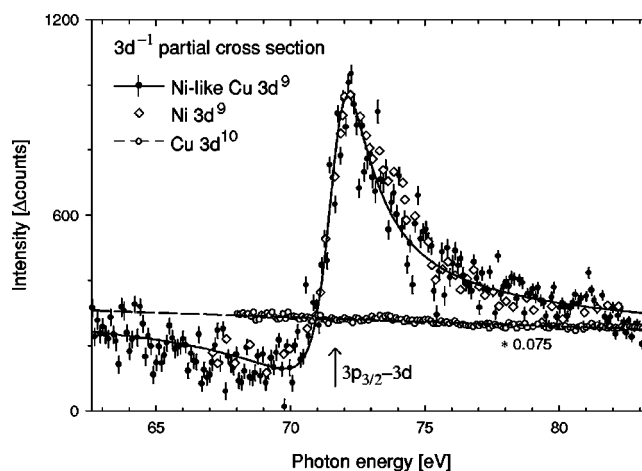
_____

[3] A CIS spectrum of the $3d^{-1}$ electron lines at $E_B = 16.9$ eV (see Fig. 3), belonging to a ^3F multiplet of the ionic $3d^8$ shell, also displays the $3p_{3/2} \rightarrow 3d$ resonance.

FIG. 4. Experimental $3d^{-1}$ partial cross sections of Ni-like Cu ($-\bullet-$, $E_B = 18.2$ eV), Ni ($\diamond$, from Ref. [25]) and Cu atoms ($--\circ--$, $E_B = 10.7$ eV) in the region of the $3p$ inner-shell excitations. The Cu spectrum was scaled by a factor of 0.075, the Ni spectrum was shifted by 9 eV to higher binding energies and scaled in order to match the Ni-like Cu spectrum. The error bars in the Ni-like Cu spectrum reflect the statistical scatter.

in good agreement with a spin-orbit splitting of 1.8 eV [27]. However, the relative strength of the $3p_{1/2} \rightarrow 3d$ component is significantly smaller than the statistical weight of 1:2, as has been noted earlier [25,26]. A transfer of this result to the Ni-like Cu atoms, additionally taking into account that the Cu* $3p_{12} \rightarrow 3d$ resonance cannot be excited from the $^2D_{5/2}$ metastable state, could explain why there is no indication of the spin-orbit partner in the spectrum of metastable Cu.

In conclusion, we have determined the emission of $3d$ electrons in the photoelectron spectrum of Cu* atoms that are laser-tailored in a metastable Ni-like $3d^9 4s^2$ state. The $3d^{-1}$ main line intensity varies strongly when the photon energy is scanned through the $3p$ thresholds. A characteristic broad and asymmetric resonance shows up in the corresponding CIS spectrum; this resonance, which can be well approximated by a Fano-type profile, is attributed to a transition of a $3p_{3/2}$ electron into the $3d$ orbital opened in the laser-tailoring process. There is no indication of a contribution from the $3p_{1/2} \rightarrow 3d$ spin-orbit partner. A detailed comparison showed that the measured CIS spectrum of the Ni-like Cu atoms is very similar to the corresponding spectrum of excited Ni $3d^9 4s$ atoms. Therefore, $3p$ photoionization of the metastable Cu atoms can serve as a model for $3p$ photoionization of Ni $3d^9 4s$ atoms. In this context it is very interesting that the photoelectron spectra of small, negatively charged Ni_n^- and Cu_n^- clusters show marked similarities indicating a strong localization of the $3d$ orbitals [28]. It would be very interesting to compare the $3p$ photoionization of metastable Cu atoms and Ni atoms bound in small clusters.

In our experiment the small number of metastable atoms precluded photoelectron spectroscopy above the $3p$ thresholds. In a future experiment, a second laser tuned to the transition between the state excited by the first laser and the metastable state will be used in order to transfer the Cu atoms more effectively from the ground state to the metastable state. Alternatively, improving the flux of the vuv light

source, as expected for example for the free-electron laser test facility TESLA at DESY [29], would bring progress.

As we have shown above, in contrast to the Cu* $3d^9 4s^2$ atoms, the $3d^{-1}$ partial cross section of the Cu $3d^{10} 4s$ ground-state atoms displays only a little resonant structure at the $3p$ threshold. Therefore resonant photoelectron spectroscopy at the $3p$ threshold offers a very sensitive test of the $3d$ shell occupation of Cu atoms or ions in compounds (see, e.g., [30–33], and references therein).

[1] P. D. Johnson, Rep. Prog. Phys. **60**, 1217 (1997).

[2] M. Liberati, G. Panaccione, F. Sirotti, P. Prieto, and G. Rossi, Phys. Rev. B **59**, 4201 (1999).

[3] J. G. Menchero, Phys. Rev. B **57**, 1001 (1998).

[4] H. A. Dürr, G. van der Laan, D. Spanke, F. U. Hillebrecht, and N. B. Brookes, J. Electron Spectrosc. Relat. Phenom. **93**, 233 (1998).

[5] C. M. Schneider, U. Pracht, W. Kuch, A. Chassé, and J. Kirschner, Phys. Rev. B **54**, R15 618 (1996).

[6] J. Stöhr, J. Electron Spectrosc. Relat. Phenom. **75**, 253 (1995).

[7] F. M. F. de Groot, J. Electron Spectrosc. Relat. Phenom. **67**, 529 (1994).

[8] A. von dem Borne, T. Dohrmann, A. Verweyen, B. Sonntag, K. Godehusen, and P. Zimmermann, Phys. Rev. Lett. **78**, 4019 (1997).

[9] K. J. Ross and B. Sonntag, Rev. Sci. Instrum. **66**, 4409 (1995).

[10] Th. Dohrmann, dissertation, Universität Hamburg, 1995.

[11] G. C. King, M. Tronc, F. H. Read, and R. C. Bradford, J. Phys. B **10**, 2479 (1977).

[12] Th. Dohrmann, A. von dem Borne, A. Verweyen, B. Sonntag, M. Wedowski, K. Godehusen, P. Zimmermann, and V. Dolmatov, J. Phys. B **29**, 4641 (1996).

[13] J. Bengtsson, J. Larsson, S. Svanberg, and C.-G. Wahlström, Phys. Rev. A **41**, 233 (1990).

[14] J. Sugar and A. Musgrove, J. Phys. Chem. Ref. Data **19**, 527 (1990).

[15] K. Fu, M. Jogwich, M. Knebel, and K. Wiesemann, At. Data Nucl. Data Tables **61**, 1 (1995).

[16] R. Bruhn, B. Sonntag, and H. W. Wolff, J. Phys. B **12**, 203 (1979).

[17] Ch. Gerth, K. Tiedtke, M. Martins, B. Obst, P. Zimmermann, P. Glatzel, A. Verweyen, Ph. Wernet, and B. Sonntag, J. Phys. B **31**, 2539 (1998).

[18] D. Chandesris, C. Guillot, G. Chauvin, J. Lecante, and Y. Petroff, Phys. Rev. Lett. **47**, 1273 (1981).

[19] R. Bruhn, E. Schmidt, H. Schröder, and B. Sonntag, J. Phys. B **15**, L441 (1982).

[20] L. C. Davis and L. A. Feldkamp, Phys. Rev. A **24**, 1862 (1981).

[21] F. Combet Farnoux, Z. Phys. D **2**, 337 (1986).

[22] B. Sonntag and P. Zimmermann, Rep. Prog. Phys. **55**, 911 (1992).

[23] L. C. Davis, J. Appl. Phys. **59**, R25 (1986).

[24] U. Fano and L. Cooper, Rev. Mod. Phys. **40**, 441 (1968).

[25] M. Meyer, Th. Prescher, E. von Raven, M. Richter, E. Schmidt, B. Sonntag, and H. Wetzel, Z. Phys. D **2**, 347 (1986).

[26] E. Schmidt, H. Schröder, B. Sonntag, and H. E. Wetzel, J. Phys. B **16**, 2961 (1983).

[27] R. E. Dietz, E. G. McRae, and J. H. Weaver, Phys. Rev. B **21**, 2229 (1980).

[28] G. Ganteför and W. Eberhardt, Phys. Rev. Lett. **76**, 4975 (1996).

[29] J. Feldhaus and B. Sonntag, Synchrotron Rad. News **11**, 21 (1998).

[30] J. Ghijsen, L. H. Tjeng, H. Eskes, G. A. Sawatzky, and R. L. Johnson, Phys. Rev. B **42**, 2268 (1990).

[31] H. Maack, diplomarbeit, Universität Hamburg, 1985.

[32] M. R. Thuler, R. L. Benbow, and Z. Hurych, Phys. Rev. B **26**, 669 (1982).

[33] M. Klauda, J. Markl, C. Fink, P. Lunz, G. Saemann-Ischenko, F. Rau, K.-J. Range, R. Seemann, and R. L. Johnson, Phys. Rev. B **48**, 1217 (1993).